

CONF-871243--9

UCRL-97950
PREPRINT

HEAVY ION COLLISIONS WITH $A = 10^{57}$:
ASPECTS OF NUCLEAR STABILITY AND THE
NUCLEAR EQUATION OF STATE IN COALESCING
NEUTRON-STAR BINARY SYSTEMS

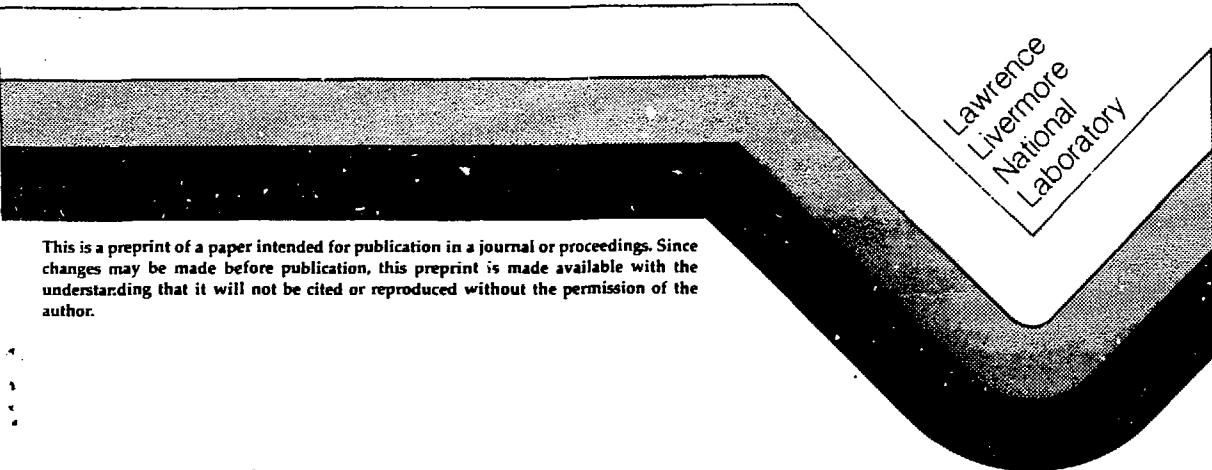
G. J. Mathews and J. R. Wilson
Lawrence Livermore National Laboratory

C. R. Evans
California Institute of Technology

S. L. Detweiler
University of Florida

This paper was prepared for
Proceedings of the Texas A&M Symposium
on Hot Nuclei
College Station, TX
7-10 December 1987

December 1987



Lawrence
Livermore
National
Laboratory

This is a preprint of a paper intended for publication in a journal or proceedings. Since changes may be made before publication, this preprint is made available with the understanding that it will not be cited or reproduced without the permission of the author.

DISTRIBUTION OF THIS DOCUMENT IS UNLIMITED

HEAVY ION COLLISIONS WITH $A = 10^5$:
ASPECTS OF NUCLEAR STABILITY AND THE NUCLEAR
EQUATION OF STATE IN COALESCING
NEUTRON-STAR BINARY SYSTEMS

G. J. Mathews and J. R. Wilson
Lawrence Livermore National Laboratory

C. R. Evans
California Institute of Technology

S. L. Detweiler
University of Florida

ABSTRACT

The dynamics of the final stages of the coalescence of two neutron stars (such as the binary pulsar PSR 1913+16) is an unsolved problem in astrophysics. Such systems are probably efficient generators of gravitational radiation, and may be significant contributors to heavy-element nucleosynthesis. The input physics for the study of such systems is similar to that required for the study of heavy-ion collision hydrodynamics; e.g., a finite temperature nuclear equation of state, properties of nuclei away from stability, etc. We discuss the development of a relativistic hydrodynamics code in three spatial dimensions for the purpose of studying such neutron-star systems. The properties of the mass-radius relation (determined by the nuclear equation of state) may lead to a proposed mechanism by which hot, highly neutronized matter is ejected from the coalescing stars. This material is photodisintegrated into a free (mostly) neutron gas which may subsequently experience rapid-neutron capture (r-process) nucleosynthesis.

By way of introduction to this talk, I am reminded of the story of the Californian visiting a Texas supermarket, who being well aware of the Texan's boast of how everything is big in Texas, commented to someone standing near the watermelons on how nice those California cucumbers were. The Texan, with a startled look, then said to the Californian, "Those aren't cucumbers, those are Texas grapes." It is appropriate, therefore, at this symposium celebrating the dedication of the new Texas A&M K500 superconducting cyclotron, that I should give a talk about

MAILED

Texas-style heavy ions. The collision rate of neutron-stars in nature is admittedly quite uncertain, although perhaps not as infrequent as one might at first presume. There is at least one good observational candidate^{1]}; the binary pulsar, PSR 1913+16, which will coalesce in a time scale of $\sim 10^8$ years.^{2]} It has also been suggested^{3]} that the short (1.5 ms) period of the millisecond pulsar^{4]} PSR 1937+214 may be the result of neutron-star coalescence, and numerical simulations^{5]} of the dynamics of dense stellar clusters suggests that the emission of gravity waves can lead to capture by passing neutron stars.

Besides the well known importance of the nuclear equation-of-state (EOS) in determining the dynamics of neutron star formation during supernovae and the neutron star limiting mass, there are two important issues in which nuclear stability and the EOS play a role in the dynamics of interacting neutron-star binary systems.^{6]} The first can be understood by reference to Fig. 1 which shows a schematic illustration^{7]} of a mass vs. radius diagram derived for a typical EOS. Important details of this figure will depend upon the EOS, however, the qualitative features will not change. Of importance for binary systems is the fact that the neutron-star radius increases with decreasing mass. This is simply because the gravitational potential decreases. Therefore, as mass transfers from the lighter to the heavier companion, the lighter companion will expand, thus increasing the mass transfer rate, and possibly leading to a dynamical instability which could disrupt the entire system. There is the potential for the release of a great deal of energy as neutron-star material approaches point B on Fig. 1.

The combination of this effect and tangential shocks caused by the merging stars may cause material to be ejected from the stars. This material could be further shock heated by the orbiting system providing enough internal energy to generate a thermal neutron star wind.^{8]}

The second point which we discuss in this paper is the role of nuclear stability as this neutron-star material is ejected

into the interstellar medium. This material may experience rapid neutron capture nucleosynthesis as it expands and cools.

We are in the process of completing a relativistic hydrodynamics code in three spatial dimensions to study the dynamics of the final stages of coalescence of such systems.^{9]}

The code we have written uses a time-explicit, Eulerian scheme which has been successfully applied to solving fully general relativistic problems in two spatial dimensions using the ADM, or 3 + 1, formalism of general relativity. We have selected a Cartesian grid since this avoids problems associated with finite differencing near coordinate singularities. In this coordinate system, the relativistic field equations assume a simpler and more symmetric form.

The equations of relativistic hydrodynamics take a form similar to their Newtonian counterpart encountered in nuclear hydrodynamics. The conservation of baryon number is given by

$$\partial_t(\gamma^{1/2}D) + \partial_i(\gamma^{1/2}DV^i) = 0 \quad (1)$$

where V^i is the usual coordinate three-velocity derived from the relativistic four-velocity U^μ and where D is related to the proper baryon number density, ρ , by $D = \rho W$ with W expressing a generalized Lorentz factor.

The equation for internal energy density is

$$\partial_t(\gamma^{1/2}E) + \partial_i(\gamma^{1/2}EV^i) = -p[\partial_t(\gamma^{1/2}W) + \partial_i(\gamma^{1/2}WV^i)] \quad (2)$$

where $E = \rho\epsilon$ and ϵ is the proper specific internal energy density. Finally, the momentum equation is found to be

$$\begin{aligned} \partial_t S_i + S_i \partial_t \ln \gamma^{1/2} + \frac{1}{\gamma^{1/2}} \partial_j (\gamma^{1/2} S_i V^j) + \\ \alpha \partial_i p + \frac{1}{2} \rho h U_j U_k \partial_i \gamma^{jk} - S_j \partial_i \beta^j + \rho h \alpha^2 \partial_i \ln \alpha = 0 \end{aligned} \quad (3)$$

where $S_i = (\rho + \epsilon + p)WU_i$ is the relativistic momentum density, p is the pressure, β_i is the ADM shift vector, α is the ADM lapse

function, and γ^{ij} is the spatial three-metric. For relativistic applications, a solution must be made for the metric quantities $\alpha, \beta_i, \gamma^{ij}$ using the field equations. Our solution to the relativistic field equations is based upon an approximation to the York-Smarr radiation gauge which gives the exact solution for stationary neutron stars although the metric is strictly conformally flat and the gravitational radiation is neglected. The solution for α, β_i and γ_{ij} can then be reduced to a set of elliptic equations.

Eventually we will need to carry up to 24 variables for each zone, including all six components of the intrinsic three-metric and the extrinsic curvature. If one wishes a resolution of $\approx 1\%$, then one requires on the order of $24 \cdot 100 \cdot 100 \cdot 100 = 2.4 \cdot 10^7$ words of memory. For our purposes, this is accommodated by using the solid state disk (SSD) for storage on the Cray X-MP/48. The evolution equations are solved by transferring two-dimensional planes sequentially between the SSD and core memory.

Although the fully relativistic version of the code with a realistic equation-of-state is not yet finished, we can gain some intuition from calculations with a polytropic EOS. Figure 2 shows three-dimensional density contours for relativistic orbiting ($I = 2$) polytropes with a mass ratio of 2/1. As the orbit of the stars approach a separation of \sim three-radii apart, an accretion flow develops. With a realistic EOS, however, a much more complicated scenario should emerge. Since material which approaches the Roche lobe is no longer gravitationally bound to be neutron-star matter, it might experience the kind of expansion instability depicted in Fig. 1. This may be a source of relativistic jets.^{10]} In any event, mass ejection should occur.

More intuition is to be gained from a recent axisymmetric two-dimensional calculation of the collision of two neutron stars.^{11]} It is interesting to note that the collision energy of such a system in free fall is about 20 MeV/nucleon when the stars collide. This is just in the optimum range of heavy-ion energies available to the new Texas A&M accelerator. Figure 3 shows a

complex pattern of shocks in a circumstellar envelope generated by the merging of the two stars. As material is repeatedly shocked, it will gain total specific energy and rise against the gravitational potential. As material moves upward at some height (as yet undetermined), a final shock will give the material net positive specific energy, launching a wind. Ejected matter reaches a terminal velocity, v_t , which may be high depending on the strength of the last shock. The decompression behavior can be quite different from (reverse) free-fall¹²); for example, a wind will satisfy $\rho t^2 \sim M/(4\pi v t^3)$, while free-fall gives $\rho t^2 \sim (6\pi G)^{-1}$. In most cases, the value of ρt^2 for a wind will be significantly less than that for reverse free-fall, indicating a more rapid dilution of the gas.

In the region below the base of the wind, repeated shocks will tend to push the matter temperature up, while the upward flow and adiabatic expansion will tend to cool the material. If the temperature rises significantly above 1 MeV, pairs are produced and degeneracy is broken. A potential problem with an r-process scenario is that matter must traverse any such high temperature region sufficiently rapidly to avoid coming into beta equilibrium due to the reactions

$$p + e^- \rightarrow n + \nu_e, \quad (4a)$$

$$n + e^+ \rightarrow p + \bar{\nu}_e. \quad (4b)$$

In high density regions, these reactions may remain blocked if neutrinos are trapped. Otherwise the n/p ratio is quickly pushed down toward unity, and an r-process would be less likely. However, even a n/p slightly greater than unity may serve to give an r-process if a large fraction of free protons quickly lock up into He. We are investigating the possibility of modeling significant aspects of the wind generation with 1D or 2D hydrodynamic simulations.

We have calculated the r-process nucleosynthesis in the framework of a classical r-process model.^{13]} In the shock-

driven wind, the density diminishes as $\rho \sim r^{-2} \sim t^{-2}$. The temperature diminishes adiabatically along with the density $T \sim \rho^{1/3}$.

To calculate the nucleosynthesis yield, one of course would require the best available estimates of nuclear properties away from stability. The calculations shown in Fig. 4 utilized the droplet model^[14] for estimating the nuclear masses away from stability, and the Klapdor beta decay rates.^[15] It appears that the calculated r-process abundance peaks occur for mass numbers below the corresponding solar system peaks. A more realistic model should produce an abundance distribution very similar to solar system r-process material. This is a calculation we are now pursuing.

This research is supported in part by NSF grants PHY83-08826 and AST85-14911 and under the auspices of the U.S. Department of Energy by the Lawrence Livermore National Laboratory under contract number W-7405-ENG-48. Some of the numerical computations were performed on the Cray X-MP at the National Center for Supercomputing Applications, University of Illinois, Urbana, Illinois.

1. Hulse, R. A. and Taylor, J. H., *Ap. J. Lett.*, 195, L51 (1975).
2. Symbalisty, E. M. D. and Schramm, D. N., *Ap. J. Lett.*, 22, 143 (1982).
3. Henrichs, H. F. and Van der Heuvel, E. P. J., *Nature*, 303, 213 (1983).
4. Backer, D. C., Kulkarni, S. R., and Taylor, J. H., *Nature*, 300, 615 (1982).
5. Kochanek, C. S., Shapiro, S. L. and Teukolski, S. A., *Ap. J.*, 320, 73 (1987).
6. Clark, J. P. A. and Eardley, D. M., *Ap. J. Lett.*, 215, 311 (1977).
7. Shapiro, S. L. and Teukolski, S. A., in "Black Holes, White Dwarfs and Neutron Stars," (Wiley, New York) (1983), p. 150.
8. Evans, C. R. and Mathews, G. J., in "Origin and Distribution of the Elements," G. J. Mathews, Ed., (World Scientific, Singapore) (1987), pp. 684-692.
9. Mathews, G. J., Wilson, J. R. and Evans, C. R., in "Advances in Nuclear Astrophysics," E. Vangioni-Flam, et al., eds. (Editions Frontieres, France) (1986) pp. 211-218.
10. Nather, R. E., in "Interacting Binaries," P. P. Eggleton and J. E. Pringle, Eds., (D. Reidel, Dordrecht) (1984) pp. 349-366.

11. Evans, C. R., Proceedings of 13th Texas Symposium on Relativistic Astrophysics, M. P. Ulmer, Ed., (World Scientific, Singapore) (1987), pp. 152-157.
12. Lattimer, J. M., Mackie, F., Ravenhall, D. G. and Schramm, D. N., Ap. J. Lett. 213, 225 (1977).
13. Mathews, G. J. and Ward, R. A., Rep. Prog. Phys., 48, 1371 (1985).
14. Myers, W. D. and Swiatecki, W. J., Ann. Phys., 84, 786 (1974).
15. Klapdor, H. V., Metzinger, J. and Oda, T., At. Data Nucl. Data Tables, 31, 81 (1984).

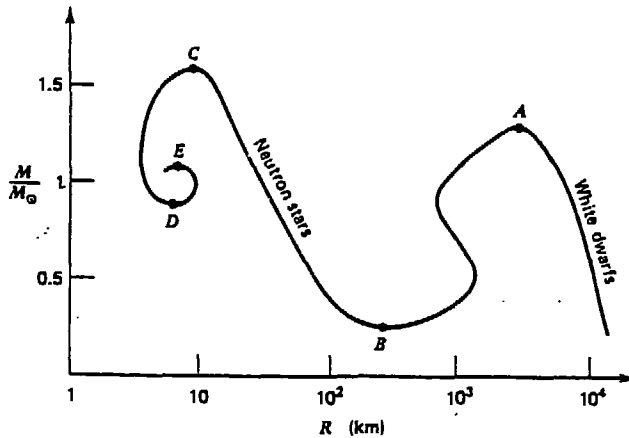


Figure 1. Schematic illustration of the mass vs. radius relation for compact objects (from Ref. 7).

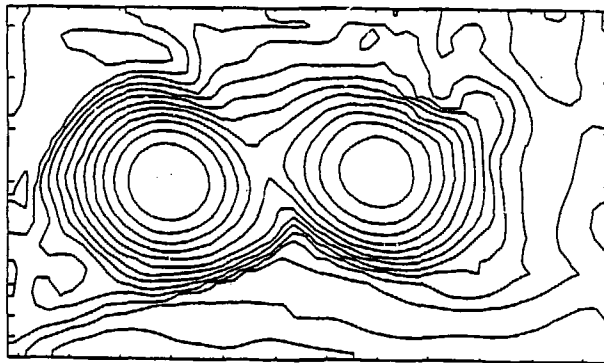


Figure 2. Logarithmic density contours through the orbital plane for two relativistic polytropic neutron stars with a mass ratio of 2/1.

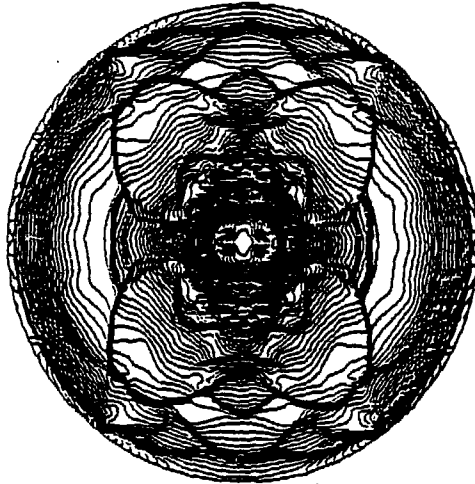


Figure 3. Contours of pressure after axisymmetric collision and merger. Collision axis is vertical. Outer boundary has a radius of 80 km. Approximately 85% of the material is within an inner core of radius ~ 20 km. Shocks driven by large amplitude oscillations and circulation within this inner, denser core are evident in the surrounding hot envelope.

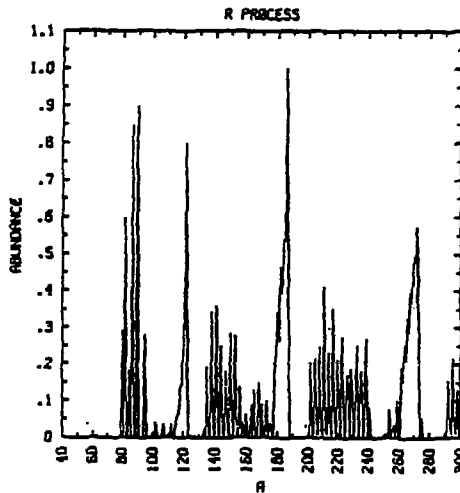


Figure 4. Calculated r-process abundances versus A, prior to decay back to stability.

DISCLAIMER

This report was prepared as an account of work sponsored by an agency of the United States Government. Neither the United States Government nor any agency thereof, nor any of their employees, makes any warranty, express or implied, or assumes any legal liability or responsibility for the accuracy, completeness, or usefulness of any information, apparatus, product, or process disclosed, or represents that its use would not infringe privately owned rights. Reference herein to any specific commercial product, process, or service by trade name, trademark, manufacturer, or otherwise does not necessarily constitute or imply its endorsement, recommendation, or favoring by the United States Government or any agency thereof. The views and opinions of authors expressed herein do not necessarily state or reflect those of the United States Government or any agency thereof.